

## On the variable timing behavior of PSR B0540–69: an almost excellent example to study pulsar braking mechanism

F. F. Kou<sup>1,2</sup>, Z. W. Ou<sup>1,2</sup> and H. Tong<sup>1</sup>

<sup>1</sup> Xinjiang Astronomical Observatory, Chinese Academy of Sciences, Urumqi 830011, China;  
tonghao@xao.ac.cn

<sup>2</sup> University of Chinese Academy of Sciences, 19A Yuquan Road, Beijing, China

**Abstract** PSR B0540–69 has braking index measurement in its persistent state:  $n = 2.129 \pm 0.012$ . Recently, it is reported to have spin-down state changes: a suddenly 36% increase in the spin-down rate. Combining the persistent state braking index measurement and different spin-down states, PSR B0540–69 is more powerful than intermittent pulsars in constraining pulsar spin-down models. The pulsar wind model is applied to explain the variable timing behavior of PSR B0540–69. The persistent state braking index of PSR B0540–69 is the combined effect of magnetic dipole radiation and particle wind. The particle density reflects the magnetospheric activity in real-time and may be responsible for the changing spin-down behavior. Corresponding to the 36% increase in the spin-down rate of PSR B0540–69, the relative increase in the particle density is 88% in the vacuum gap model. And the model calculated braking index in the new state is  $n = 1.79$ . Future braking index observation of PSR B0540–69 in the new spin-down state will be very powerful in distinguishing between different pulsar spin-down models and different particle acceleration models in the wind braking scenario. The variable timing behavior of PSR J1846–0258 is also understandable in the pulsar wind model.

**Key words:** pulsars: general – pulsars: individual (PSR B0540–69; PSR J1846–0258)  
– stars: neutron – wind

### 1 INTRODUCTION

PSR B0540–69, known as the “Crab Twin”, is a young radio pulsar with spin-down parameters  $\nu \approx 19.727$  Hz,  $\dot{\nu} \approx -1.86 \times 10^{-10}$  Hzs<sup>-1</sup> (Marshall et al. 2015) and braking index  $n = 2.129 \pm 0.012$  (Ferdman et al. 2015). Its characteristic magnetic field is about  $10^{13}$  G at the magnetic poles<sup>1</sup>. Only two glitches with relative small changes in spin-down parameters were reported (Zhang et al. 2001; Cusumano et al. 2003; Livingstone et al. 2005; Ferdman et al. 2015). Recently, a persistent and unprecedented increase in the spin-down rate of PSR B0540–69 was observed: the relative increase in the spin-down rate is 36% which is orders magnitude larger than the changes induced by glitches (Marshall et al. 2015). Another pulsar PSR J1846–0258 was also reported to have variable timing behaviors: a net decrease in the spin frequency ( $\Delta\nu \approx -10^4$  Hz) after the large glitch (Livingstone et al. 2010) and a lower braking index  $n = 2.19 \pm 0.03$  (Livingstone et al. 2011; Archibald et al. 2015b) than its persistent state value  $n = 2.65 \pm 0.01$  (Livingstone et al. 2006).

The spin-down behavior of pulsars can be described by the power law:

$$\dot{\nu} = -C\nu^n, \quad (1)$$

<sup>1</sup> Assuming all the rotational energy is consumed by magneto-dipole radiation in vacuum,  $B(\text{pole}) = 6.4 \times 10^{19} \sqrt{P\dot{P}}$  G

**Table 1** Comparison of spin-down parameters of PSR B1931+24, PSR B0540–69, and PSR J1846–0258. The intermittent pulsar PSR B1931+24 has different spin-down states without any braking index information at present. PSR B0540–69 has both different spin-down states and the persistent state braking index measurement. PSR J1846–0258 is reported to have a variation of braking index.

| Pulsar name                                | $\nu$ (Hz) | $\dot{\nu}$ (Hz s <sup>-1</sup> ) | braking index      |
|--|------------|-----------------------------------|--------------------|
| B1931+24 (off) <sup>a</sup>                | 1.229      | $-10.8 \times 10^{-15}$           | ?                  |
| B1931+24 (on) <sup>a</sup>                 | 1.229      | $-16.3 \times 10^{-15}$           | ?                  |
| B0540–69 (low) <sup>b</sup>                | 19.727     | $-1.86 \times 10^{-10}$           | 2.129 <sup>c</sup> |
| B0540–69 (high) <sup>b</sup>               | 19.701     | $-2.53 \times 10^{-10}$           | ?                  |
| J1846–0258 (persistent state) <sup>d</sup> | 3.08       | $-6.72 \times 10^{-11}$           | 2.65               |
| J1846–0258 (after glitch) <sup>e</sup>     | 3.06       | $-6.65 \times 10^{-11}$           | 2.19               |

(a): From Kramer et al. (2006). The on state has larger spin-down rate than the off state.

(b): From Marshall et al. (2015). “Low” means the previous spin-down state and “high” means the new spin-down state with a higher spin-down rate.

(c) Mean value of braking index (Ferdman et al. 2015).

(d) From Livingstone et al. (2006).

(e) From Archibald et al. (2015b).

where  $\nu$  and  $\dot{\nu}$  are respectively the spin frequency and frequency derivative,  $C$  is usually taken as a constant and  $n$  is the braking index. The braking index is defined accordingly:

$$n = \frac{\nu\ddot{\nu}}{\dot{\nu}^2}, \quad (2)$$

where  $\ddot{\nu}$  is the second derivative of spin frequency. The braking index reflects the pulsar braking mechanism (Tong 2015). In the magneto-dipole braking model, a pulsar rotates uniformly in vacuum  $\dot{\nu} \propto \nu^3$ . The expected braking index is three which is not consistent with the observations (Lyne et al. 2015). Like the intermittent pulsar (Kramer et al. 2006), PSR B0540–69 also has two different spin-down states. For the intermittent pulsar PSR B1931+24, people tried to measure its braking index during the on and off state (Young et al. 2013). Now this aim has been partially fulfilled by PSR B0540–69 which has not only different spin down states but also braking index measurement for the persistent state (“low” spin-down rate state), see Table 1. Therefore, it can put more constraints on pulsar spin-down models. Any candidate model should explain both the braking index during the persistent state and the variable spin-down rate.

Previously, the pulsar wind model (Xu & Qiao 2001) is employed to explain the spin-down behavior of intermittent pulsars (Li et al. 2014) and braking index of the Crab pulsar (Kou & Tong 2015). In the following, it is shown that both the persistent state braking index and varying spin-down rate of PSR B0540–69 are understandable in the wind braking model. The varying spin-down rate is due to a variable particle wind. And the varying braking index of PSR J1846–0258 is caused by a changing particle density. The pulsar wind model and calculations are listed in Section 2. Discussions and conclusions are presented in Section 3 and Section 4, respectively.

## 2 VARIABLE TIMING BEHAVIOR OF PULSARS CAUSED BY A VARYING PARTICLE WIND

### 2.1 Description of the pulsar wind model

Pulsars are oblique rotators in general. The perpendicular and parallel magnetic dipole moment may respectively relate to the magnetic dipole radiation and particles acceleration (Xu & Qiao 2001; Kou & Tong 2015):

$$\dot{E}_d = \frac{2\mu^2\Omega^4}{3c^3} \sin^2 \alpha, \quad (3)$$

$$\dot{E}_p = 2\pi r_p^2 c \rho_e \Delta\phi = \frac{2\mu^2 \Omega^4}{3c^3} 3\kappa \frac{\Delta\phi}{\Delta\Phi} \cos^2 \alpha, \quad (4)$$

where  $\mu = 1/2BR^3$  is the magnetic dipole moment ( $B$  is the polar magnetic field and  $R$  is the neutron star radius),  $c$  is the speed of light, and  $\alpha$  is the angle between the rotational axis and the magnetic axis (i. e., inclination angle),  $\Omega = 2\pi\nu$  is the angular velocity of the pulsar,  $r_p = R(R\Omega/c)^{1/2}$  is the polar cap radius,  $\rho_e = \kappa\rho_{\text{GJ}}$  is the primary particle density where  $\rho_{\text{GJ}} = \Omega B/(2\pi c)$  is the Goldreich-Julian charge density (Goldreich & Julian 1969) and  $\kappa$  is the dimensionless particle density,  $\Delta\phi$  is the corresponding acceleration potential of the acceleration region, and  $\Delta\Phi = \mu\Omega^2/c^2$  is the maximum acceleration potential for a rotating dipole (Ruderman & Sutherland 1975). The pulsar rotational energy is consumed by the combined effect of magnetic dipole radiation and particle acceleration (Xu & Qiao 2001)

$$-I\Omega\dot{\Omega} = \frac{2\mu^2\Omega^4}{3c^3}\eta, \quad (5)$$

where  $I = 10^{45} \text{ g cm}^2$  is the moment of inertia, and

$$\eta = \sin^2 \alpha + 3\kappa\Delta\phi/\Delta\Phi \cos^2 \alpha. \quad (6)$$

The spin-down behavior can be expressed as:

$$\dot{\Omega} = -\frac{2\mu^2\Omega^3}{3Ic^3}\eta. \quad (7)$$

According the equation (2), the braking index in the pulsar wind model can be written as (Xu & Qiao 2001):

$$n = 3 + \frac{\Omega}{\eta} \frac{d\eta}{d\Omega}, \quad (8)$$

The exact expression of  $\eta$  (equation (6)) depends on the particle acceleration potential. The vacuum gap model (Ruderman & Sutherland 1975) is taken as an example to show the calculation process and

$$\eta = \sin^2 \alpha + 4.96 \times 10^2 \kappa B_{12}^{-8/7} \Omega^{-15/7} \cos^2 \alpha, \quad (9)$$

where  $B_{12}$  is the magnetic field in units of  $10^{12} \text{ G}$  (Kou & Tong 2015). For other acceleration models, the corresponding expressions of  $\eta$  are listed in Table 2 in Kou & Tong (2015).

## 2.2 On the variable timing behavior of PSR B0540–69

A generic picture for the variable timing behavior of PSR B0540–69 and PSR J1846–0258 is: a glitch may occurred during the observations, as that in PSR J1846–0258 (Livingstone et al. 2010). This small glitch may have been missed in the case of PSR B0540–69. This glitch may induce some magnetospheric activities, e.g., outburst (Gavriil et al. 2008). The particle outflow will be stronger during this process. This will cause the pulsar to have a larger spin-down rate (Marshall et al. 2015). After some time, a larger spin-down state will result in a net spin-down of the pulsar compared with previous timing solutions (Livingstone et al. 2010). The braking index will be smaller since the particle wind is stronger (Wang et al. 2012a). When the pulsar magnetosphere relax to its persistent state, if the particle density is still varying with time  $\kappa = \kappa(t)$ , the braking index will be different with the persistent state while the change in spin-down rate may be neglected (Livingstone et al. 2011; Archibald et al. 2015b; Kou & Tong 2015). From previous observations of PSR J1846–0258, its pulse profile has no significant variations before, during and after the outburst (Livingstone et al. 2010, 2011; Archibald et al. 2015b). The observations of magnetar 1E 1048.1–5937 showed that the pulsed flux may not be a good indicator of the magnetospheric activities (Archibald et al. 2015a). The variation of total X-ray flux is needed. Therefore, the enhanced spin-down rate in PSR B0540–69 without changes in pulse profile and pulsed

**Table 2** Braking indices of PSR B0540–69 in the new state in all the acceleration models.

| Acceleration models | VG(CR) | VG(ICS) | SCLF(IL,CR) | SCLF(I) | OG   | CAP  | NTVG(CR) | NTVG(ICS) |
|---------------------|--------|---------|-------------|---------|------|------|----------|-----------|
| Braking index       | 1.79   | 1.87    | 1.90        | 1.79    | 1.38 | 1.83 | 1.90     | 1.86      |

Notes: See Table 2 of Kou & Tong 2015 for the meanings of the acceleration models abbreviations. The minimum braking index of the SCLF (II ICS) is 2.4 (Li et al. 2014) which is larger than the persistent braking index of PSR B0540–69:  $n = 2.129$ . It means that the SCLF (II, ICS) model can be ruled out or can not exist alone to accelerate particle in the magnetosphere of PSR B0540–69 (Wu et al. 2003; Li et al. 2014).

flux is not unusual (Marshall et al. 2015). The reason may be that the geometry of the pulsar is unchanged during the magnetospheric activities. This may result in a constant pulse profile and pulsed flux.

For PSR B0540–69, giving the persistent state spin-down parameters  $\nu = 19.727$  Hz,  $\dot{\nu} = -1.86 \times 10^{-10}$  Hz s $^{-1}$  (Marshall et al. 2015), and inclination angle  $\alpha = 50^\circ$  (the best fitted value given by Zhang & Cheng 2000). Parameters of magnetic field  $B = 10^{13}$  G and  $\kappa = 834$  can be calculated (by solving equations (5) and (8)) corresponding to the observed braking index  $n = 2.129 \pm 0.012$  (Ferdman et al. 2015). The calculated  $\kappa = 834$  means that the particle density is 834 times the Goldreich-Julian charge density which is consistent with previous conclusions (Kou & Tong 2015 and references therein).

The spin-down rate of PSR B0540–69 has increased by 36% in the new spin-down state (Marshall et al. 2015). In the pulsar wind model, the variation of the spin-down rate is caused by a different particle density

$$\frac{\dot{\Omega}'}{\dot{\Omega}} = \frac{\eta(\kappa')}{\eta(\kappa)}, \quad (10)$$

where  $\dot{\Omega}'$  and  $\eta(\kappa')$  correspond to the new spin-down state. A larger particle density will result in a higher spin-down rate (equation(7) and (9)). Figure 1 and figure 2 shows respectively the normalized spin-down rate  $\dot{\nu}'/\dot{\nu}$  and braking index as function of normalized particle density  $\kappa'/\kappa$  for PSR B0540–69 in the vacuum gap model. As shown in figure 1, the spin-down rate increases as the particle density increases. An increase in the particle density of 88% will result in the 36% increase in the spin-down rate. As particle density increase, the braking index will decrease because the effect of particle wind component is increasing (figure 2). When the particle density increases to 1.88 times the previous value, the braking index decreases to 1.79, the relative change is 15.7%. And the corresponding frequency second derivative will be  $\ddot{\nu} = 5.83 \times 10^{-21}$  Hz s $^{-2}$  (equation (2)).

Calculations in all the acceleration models are also made. The same conclusion is obtained from these models: an increasing particle density results in the increase in spin-down rate. For PSR B0540–69, corresponding to the observational 36% relative increase in spin-down rate, the relative increase in the particle density in all these models ranges from 72% to 154%. The second frequency derivative ranges from  $4.5 \times 10^{-21}$  Hz s $^{-2}$  to  $6.15 \times 10^{-21}$  Hz s $^{-2}$ . Braking indices in the new state in all these acceleration models are list in Table 2. If the conversion efficiency of particle energy to X-ray luminosity is unchanged (Becker 2009), the total X-ray luminosity may also have increased by the same factor.

### 2.3 On the variable timing behaviors of PSR J1846–0258

Spin-down parameters and persistent state braking index of PSR J1846–0258 are respectively:  $\nu = 3.08$  Hz and  $\dot{\nu} = -6.72 \times 10^{-11}$  Hz s $^{-1}$  and  $n = 2.65 \pm 0.01$  (Table1) (Livingstone et al. 2006). In the pulsar wind model, corresponding to the observational braking index, the magnetic field  $B = 1.25 \times 10^{14}$  G and particle density  $\kappa = 28$  are calculated in the vacuum gap model with an inclination angle  $45^\circ$  (a inclination angle of  $45^\circ$  is chosen in the following calculations<sup>2</sup>). Such a magnetic field is comparable with the characteristic magnetic field  $9.7 \times 10^{13}$  G at the poles and much larger than

<sup>2</sup> There is no observational or best fitted inclination angle given.

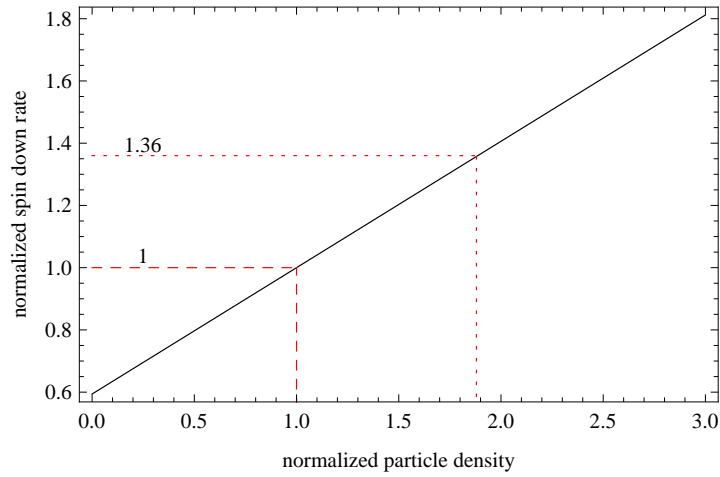


**Fig. 1** The normalized spin-down rate as function of the normalized particle density for PSR B0540–69 in the vacuum gap model. The dashed line is the spin-down rate in the persistent state. The dotted line is the new spin-down rate which is 1.36 times the persistent state spin-down rate (Marshall et al. 2015).

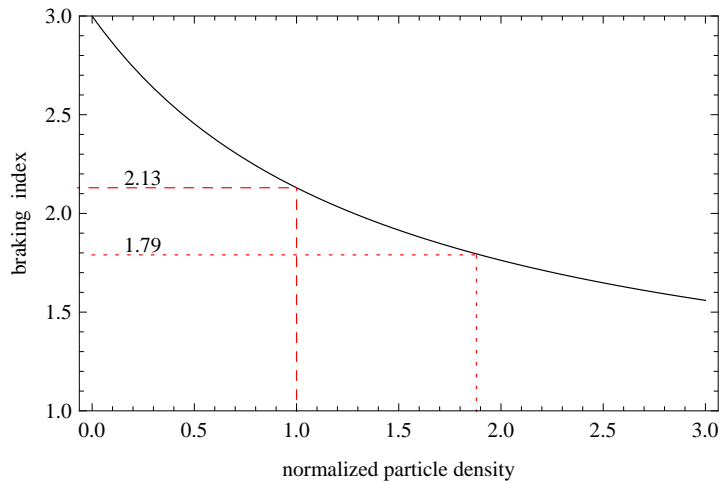


**Fig. 2** Braking index as function of the normalized particle density for PSR B0540–69 in the vacuum gap model. The dashed line is the persistent state braking index 2.13 (Ferdman et al. 2015). The dotted line is the braking index 1.79 which is predicted by the increased particle density.

magnetic fields of normal pulsars. Then it is not surprising that magnetar activities can be observed in this source (Gavriil et al. 2008).

Variable timing behavior of a net decrease in the spin-down frequency ( $\Delta\nu \approx -10^{-4}$  Hz) was detected for PSR J1846–0258 after a larger glitch (Livingstone et al. 2010). The correspondingly relative increase in the spin-down rate is about 7% ( $\Delta\dot{\nu} = -4.82 \times 10^{-12}$  Hz s $^{-1}$  during an epoch 240 days when phase coherency is lost). Such an increase in spin down rate may also be caused by a larger

particle density. Just like the calculation for PSR B0540–69, in the vacuum gap model of the pulsar wind model, a 44% increase in the particle density results in the 7% increase in the spin-down rate. The braking index will also be smaller during this enhanced spin-down epoch. However, braking index measurement is only available long after the glitch when the timing noise is greatly reduced.

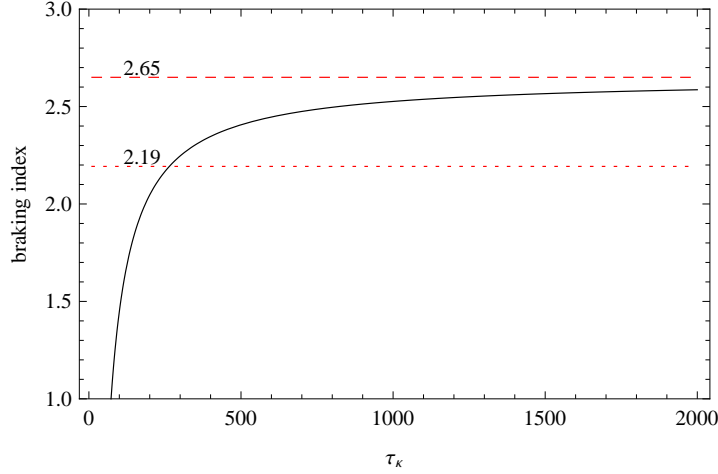


**Fig. 3** The braking index of the PSR J1846–0258 as function of  $\tau_\kappa$  in the vacuum gap model. The dashed line is the persistent state braking index 2.65 (Livingstone et al. 2006). The dotted line is the smaller braking index 2.19 measured after the glitch (Archibald et al. 2015b).

A lower braking index  $2.19 \pm 0.03$  is detected after the glitch (Livingstone et al. 2011; Archibald et al. 2015b) which is significantly smaller than its persistent state value  $n = 2.65 \pm 0.01$  (Livingstone et al. 2006). In the pulsar wind model, it can be understood by a time varying particle density  $\kappa = \kappa(t)$  (similar to the Crab pulsar, Kou & Tong 2015):

$$n = 3 + \frac{\Omega}{\eta} \frac{d\eta}{d\Omega} - \frac{\kappa}{\eta} \frac{d\eta}{d\kappa} \frac{\tau_c}{\tau_\kappa}, \quad (11)$$

where  $\tau_c = -\frac{\Omega}{2\dot{\Omega}}$  is the characteristic age,  $\tau_\kappa = \frac{\kappa}{2\dot{\kappa}}$  is the typical variation timescale of the particle density. An increasing particle density ( $\tau_\kappa > 0$  or  $\dot{\kappa} > 0$ ) lead to a smaller braking index. From figure 3, the braking index is insensitive to  $\tau_\kappa$  when it is much larger than 1000 yr, but decrease sharply when  $\tau_\kappa$  is comparable with the characteristic age (about 700 yr). The changing rate of the particle density  $\dot{\kappa} = 1.68 \times 10^{-9} \text{ s}^{-1}$  will result in a braking index of 2.19. During the epoch from MJD 55369 to MJD 56651, the particle density has increased 0.66%. The relative increase in spin-down rate is 0.1% which is very small. Therefore, the changing particle density will mainly result in a different braking index while not affecting the spin-down rate. This is the difference between the variable timing behavior of PSR 0540–69 and PSR J1846–0258.

### 3 DISCUSSIONS

Observations of intermittent pulsars (Kramer et al. 2006) and measurement of braking indices (Lyne et al. 2015) help to distinguish between different pulsar spin-down mechanisms. The variable spin-down rate of PSR B0540–69 combined with its persistent state braking index measurement is more powerful than intermittent pulsars in constraining different models. In the magneto-dipole radiation model  $\dot{\nu} \propto \mu^2 \sin^2 \alpha / I \times \nu^3$ , in order to explain the braking indices ( $n < 3$ ) of eight young pulsars, an increasing inclination angle (Lyne et al. 2013), increasing magnetic field (Espinoza et al. 2011) or

decreasing moment of inertia (Yue et al. 2007) is expected. The variable spin-down rate may be induced by the change of inclination angle, magnetic field or moment of inertia. Corresponding to the 36% relative increase in the spin-down rate, the relative change should be: 26% increase in inclination angle, or 17% increase in magnetic field, or 26% decrease in moment of inertia. It seems impossible to achieve such huge changes during a short timescale (about 14 days, Marshall et al. 2015). A change in inclination angle is unlikely since the pulse profile did not change significantly (Marshall et al. 2015). An increase in magnetic field will require an increase of magnetic energy by 36%, about  $10^{42}$  erg. It is unlikely there is such a huge amount of energy injection. A decrease of moment of inertia will require a decrease of neutron star radius. During this process, a huge amount of gravitational energy will be released (Zhou et al. 2014), about  $10^{52}$  erg, which is again unlikely.

Previous models for the spin-down behavior of intermittent pulsars (Beskin & Nokhrina 2007; Li et al. 2012) may also be applied to the variable spin-down rate of PSR B0540–69. However, the expected braking index is three in Beskin & Nokhrina (2007) and the magnetohydrodynamical simulations (Li et al. 2012). Considering the effect of pulsar death or evolution of inclination angle, the braking index will be larger than three (Contopoulos & Spitkovsky 2006; Philippov et al. 2014). Therefore, these models should be modified before they can explain both the persistent state braking index and variable spin-down rate of PSR B0540–69.

There are several models designed for magnetar spin-down which may also be employed to the case of PSR B0540–69. The magnetar spin-down may be dominated by a particle wind (Harding et al. 1999). The calculations in Harding et al. (1999) is equivalent to assuming each outflow particle can attain the maximum acceleration potential of a rotating dipole (Tong et al. 2013). This wind braking model of magnetars was employed by Kramer et al. (2006) to explain the spin-down behavior of the first intermittent pulsar PSR B1931+24. An additional particle outflow in the on state will result in a larger spin-down rate. The rotational energy loss is related to the particle wind luminosity  $L_p$  as  $\propto \sqrt{L_p}$  (Harding et al. 1999). A particle wind luminosity 85% larger will result in a spin-down rate 36% larger. The particle wind luminosity is related to the polar cap radius  $R_{pc}$  and magnetospheric opening radius  $r_{open}$  as  $L_p \propto R_{pc}^4 \propto r_{open}^{-2}$  (Harding et al. 1999). Therefore, the magnetospheric opening radius will be 26% smaller. However, there are several problems when applying the wind braking model of magnetars to the case of normal pulsars: (1) In the wind braking model of magnetars, a strong particle wind is assumed. The effect of magnetic dipole radiation is neglected. This may be applicable to the case of magnetars whose emissions are dominated by magnetic energy output (Tong et al. 2013). However, in the case of normal pulsars (including intermittent pulsars) the effect of dipole radiation may not be neglected. (2) In the case of strong particle wind, the braking index is  $n = 1$  (Tong et al. 2013). This is not consistent with the braking index of pulsars (Lyne et al. 2015). (3) When applying to the case of intermittent pulsars (Kramer et al. 2006; Young et al. 2013), pure magnetic dipole braking is assumed for the off state. This may be valid for the case of intermittent pulsars whose radio emissions are stopped in the off state (Li et al. 2014). However, this assumption can not be applied to the persistent spin-down state of PSR B0540–69 which still has multiwave emissions.

The twisted magnetosphere model of magnetars (Thompson et al. 2002) showed that the effective magnetic field will be larger for a larger twist. If the magnetosphere of PSR B0540–69 is twisted by a glitch, then it will also result in a larger spin-down rate. However, the twisted magnetosphere will relax back to the pure magnetic dipole case in several years (Beloborodov 2009). During this process, the neutron star X-ray luminosity, spin-down rate will both decrease with time. For PSR B0540–69, its high spin-down state has lasted more than 3 years (Marshall et al. 2015). This is inconsistent with the expectation of the twisted magnetosphere model.

There are also external models for the braking index or intermittent pulsar spin-down behavior, e.g., the fallback disk model (Liu et al. 2014 and references therein; Li et al. 2006). However, these external models are hard to verify or falsify. Furthermore, accretion will halt the magnetospheric activities. In the presence of accretion, it may be difficult to reconcile with the radio emissions in PSR B0540–69 and in other pulsars with braking index measured.

Observations of the timing behavior and pulse profile of some pulsars indicate that the  $\dot{\nu}$  modulation and the pulse-shape variation are correlated, e.g., PSR B0910+16 (Perera et al. 2015a) and PSR

B1859+07 (Perera et al. 2015b). The connection indicates that both these phenomena are magnetospheric origin (Lyne et al. 2010). Theory of a variable particle density in the magnetosphere is successfully applied to explain the spin-down behavior and emission property of the intermittent pulsar (Kramer et al. 2006; Li et al. 2014). The mode changing and nulling pulsar may be understood similarly because of the detection of variation in spin-down rate of PSR J1717–4054 (Young et al. 2015) and a weak emission state in addition to its bright and nulling states of PSRs J1853+0505 and J1107-5907 (Young et al. 2014). For PSR B0540–69, the increase of particle density in the magnetosphere will change the spin-down rate, as well as the pulse profile. The radio giant pulse of PSR B 0540–69 (Johnston et al. 2004) may be caused by a larger out-flowing particle density. Besides, different emission models (core, cone and patch) are applied to explain the variable mean pulse profiles (Lyne & Manchester 1988). And, it is predicted that the corotation of magnetosphere with pulsar may also affects the emission properties (Wang et al. 2012b). Hence, the nonuniform distribution of particles between these core and conal components will change the pulse shape also. For PSR B0540–69, the pulse profile has a broad double peak which can be described with two Gaussians with a phase separation of 20% (de Plaa et al. 1993). We could emphasize that: (i) if the particles distribute uniform, the increase in out-flowing particle density may result in the increase of pulse intensity, the ratio of these two component keeps constant; (ii) if the particles distribute nonuniform, both the pulse intensity and the ratio will change; (iii) the coherent manner of radiated particles may affect the pulse shape as well. The pulse profile and total flux in the high spin-down state are needed to compare with them in the low spin-down state.

#### 4 CONCLUSIONS

The pulsar wind model is applied to explain the variable timing behavior of PSR B0540–69 and PSR J1846–0258. Both the persistent state braking index and the variable spin-down rate of PSR B0540–69 are understandable. A larger particle density will result in an increase in the spin down rate and predicts a smaller braking index. And an increasing particle density will lead to a lower braking index. For PSR B0540–69, in the vacuum gap model, corresponding to the 36% increase in the spin-down rate, the relative increase in particle density is 88%. And the braking index decreases to 1.79. The same conclusion is obtained for the different acceleration models. Since it has both a variable spin-down rate and persistent state braking index measured, PSR B0540–69 is very powerful in constraining different pulsar spin-down mechanisms. Future observation of braking index in the new spin-down state will provide further test on different spin-down models and different particle acceleration models in the wind braking scenario. For PSR J1846–0258, the variable timing behavior of a net decreasing in spin down frequency ( $\Delta\nu \approx -10^{-4}$  Hz) can be understood similarly. And a changing rate of particle density  $\dot{\kappa} = 1.68 \times 10^{-9} \text{ s}^{-1}$  will result in the lower braking index 2.19.

#### ACKNOWLEDGMENTS

The authors would like to thank R.X.Xu for discussions. H.Tong is supported West Light Foundation of CAS (LHXZ201201), 973 Program (2015CB857100) and Qing Cu Hui of CAS.

#### References

- Archibald R. F., Kaspi V. M., Ng C. Y., et al., 2015a, *ApJ*, 800, 33
- Archibald R. F., Kaspi V. M., Beardmore A. P., et al., 2015b, arXiv:1506.06104
- Becker W., 2009, *Neutron stars and pulsars*, *ASSL*, 357, 91
- Beloborodov A. M., 2009, *ApJ*, 703, 1044
- Beskin V. S., & Nokhrina E. E., 2007, *Ap&SS*, 308, 569
- Contopoulos I., & Spitkovsky A., 2006, *ApJ*, 643, 1139
- Cusumano G., Massaro E., & Mineo T., 2003, *A&A*, 402, 647
- de Plaa J., Kuiper L., Hermsen W., 2003, *A&A*, 400, 1013



- Espinoza C. M., Lyne A. G., Kramer M., et al., 2011, *ApJ*, 741, L13
- Ferdamn R. D., Archibald R. F., & Kaspi, V. M. 2015, arXiv:1506.00182
- Gavriil F. P., Gonzalez M. E., Gotthelf E. V., et al., 2008, *Science*, 319, 1802
- Goldreich P., & Julian W. H., 1969, *ApJ*, 157, 869
- Harding A. K., Contopoulos I., & Kazanas D., 1999, *ApJ*, 525, L125
- Johnston S., Romani R. W., Marshall F. E., et al., 2004, *MNRAS*, 355, 31
- Kou F. F. & Tong H., 2015, *MNRAS*, 450, 1990
- Kramer M., Lyne A. G., O'Brien J. T., et al., 2006, *Science*, 312, 549
- Li J., Spitkovsky A., & Tchekhovskoy A., 2012, *ApJL*, 746, L24
- Li L., Tong H., Yan W. M., et al., 2014, *ApJ*, 788, 16
- Li X. D., 2006, *ApJ*, 646, L139
- Liu X. W., Xu R. X., Qiao G. J., et al., 2014, *RAA*, 14, 85
- Livingstone M. A., Kaspi V. M., & Gavriil F. P., 2005, *ApJ*, 633, 1095
- Livingstone M. A., Kaspi V. M., Gotthelf E. V., et al., 2006, *ApJ*, 647, 1286
- Livingstone M. A., Kaspi V. M., & Gotthelf E. V., 2010, *ApJ*, 710, 1710
- Livingstone M. A., Ng C.-Y., Kaspi V. M., et al., 2011, *ApJ*, 730, 66
- Lyne A. G., Manchester R. N., 1988, *MNRAS*, 234, 477
- Lyne A., Hobbs G., Kramer M., Stairs I., Stappers B., 2010, *Science*, 329, 408
- Lyne A. G., Smith F. G., Weltevrede P., et al., 2013, *Science*, 342, 598
- Lyne A. G., Jordan C. A., Smith F. G., et al., 2015, *MNRAS*, 446, 857
- Marshall F. E., Guillemot L., Harding A. K., et al., 2015, *ApJ*, 807, L27
- Perera B. B. P., Stappers B. W., Weltevrede P., et al., 2015a, 446, 1380
- Perera B. B. P., Stappers B. W., Weltevrede P., et al., 2015b, arXiv: 151004484
- Philippov A., Tchekhovskoy, A., & Li J. G., 2014, *MNRAS*, 441, 1879
- Ruderman M. A., & Sutherland P. G., 1975, *ApJ*, 196, 51
- Thompson C., Lyutikov M., & Kulkarni S. R., 2002, *ApJ*, 574, 332
- Tong H., 2015, arXiv:1506.04605
- Tong H., Xu R. X., Song L. M., et al., 2013, *ApJ*, 768, 144
- Wang J., Wang N., Tong H., et al., 2012, *Astrophys.Space Sci.*, 340, 307
- Wang P. F., Wang C., & Han J. L., 2012b, *MNRAS*, 423, 2464
- Wu F., Xu R. X., & Gil J., 2003, *A&A*, 409, 641
- Xu R. X., & Qiao G. J., 2001, *ApJ*, 561, L85
- Young N. J., Stappers B. W., Lyne A. G., et al., 2013, *MNRAS*, 429, 2569
- Young N. Y., Weltevrede P., Stappers B. W., et al., 2014, 442, 2519
- Young N. Y., Weltevrede P., Stappers B. W., et al., 2015, 449, 1495
- Yue Y. L., Xu R. X., & Zhu W. W., 2007, *Advance in Space Research*, 40, 1491
- Zhang L., & Cheng, K. S., 2000, *A&A* 363, 575
- Zhang W., Marshall F. E., Gotthelf E. V., et al., 2001, *ApJ*, 554, L177
- Zhou E. P., Lu J. G., Tong H., et al., 2014, *MNRAS*, 443, 2705